

Supporting Information

Near-Infrared Zn-Doped Cu₂S Quantum Dots: An Ultrasmall Theranostic Agent for Tumor Cell Imaging and Chemodynamic Therapy

Shulan Li^a, Peng Jiang^{b,*}, Siyu Hua^a, Feng-Lei Jiang^a, Yi Liu^{a,c,d,*}

^a Department of Chemistry & Sauvage Center for Molecular Sciences, College of Chemistry
and Molecular Sciences, Wuhan University, Wuhan 430072, P. R. China

^b Key Laboratory of Combinatorial Biosynthesis and Drug Discovery (Wuhan University),
Ministry of Education, and Wuhan University School of Pharmaceutical Sciences, Wuhan
430071, China.

^c Institute of Advanced Materials and Nanotechnology & Key Laboratory of Coal Conversion
and New Carbon Materials of Hubei Province, College of Chemistry and Chemical
Engineering, Wuhan University of Science and Technology, Wuhan 430081, P. R. China

^d State Key Laboratory of Membrane Separation and Membrane Process, College of
Chemistry and Chemical Engineering & College of Environmental Science and Engineering,
Tiangong University, Tianjin 300378, P. R. China.

*Correspondence to E-mail: yiliuchem@whu.edu.cn or jiangpeng@whu.edu.cn

Supporting Information – Table of Contents

Contents	Page
Effects of different reaction conditions on the PL intensity of Cu ₂ S and Zn:Cu ₂ S QDs.	4
Figure S1. The effects of synthesis condition on the fluorescence of Cu ₂ S QDs.	5
Figure S2. The effects of synthesis condition on the fluorescence of Zn:Cu ₂ S QDs.	6
Figure S3. The additional characterization of Cu ₂ S and Zn:Cu ₂ S QDs (TEM, XRD, EDX, HRTEM).	7
Figure S4. The additional XPS spectra of Cu ₂ S and Zn:Cu ₂ S QDs.	7
First-order reaction integral rate equation function.	8
Lifetime bi-exponential function.	8
Figure S5. Intracellular Cu contents of SGC-7901, HL-60 and 3T3, COS7 cells treated with Cu ₂ S QDs for 24 h	8
Figure S6. MTT results with QDs incubation.	9
Figure S7. OPDA for in vitro •OH detection and ROS detection of SGC-7901 cells after Zn:Cu ₂ S QDs incubation.	10
Figure S8. Apoptosis results after incubated with QDs.	10
Figure S9. Mitochondrial membrane potential results after incubated with QDs.	11
Table S1. Mitochondrial transmembrane potential assay of Cu ₂ S QDs.	11
Figure S10. Flow cytometry analysis cycle of SGC-7901.	12
Figure S11. Flow cytometry analysis AO staining of SGC-7901.	12
Figure S12. Flow cytometry analysis MDC staining of SGC-7901.	13
Figure S13. Western blot analysis of P62 protein in SGC-7901 cells.	13

Figure S14. LysoSensor-Green staining of SGC-7901 cells.	14
Figure S15. Confocal microscopy analysis of LysoSensor-Green stained SGC-7901 cells	14
Figure S16. Hematological assay.	15
Figure S17. Histological analyses of the major tissues for systemic toxicity analysis.	15

Effects of different reaction conditions on the PL intensity of Cu₂S and Zn:Cu₂S QDs

The effects of different reaction conditions on the fluorescence intensity were investigated to improve the luminescence properties of Cu₂S QDs. As shown in Figure S1a and 1b, the PL emission intensity of Cu₂S QDs significantly increased with the increased of Cu²⁺/thiourea ratio, reaching a maximum when the ratio was 1:1. However, if the Cu²⁺/thiourea ratio is further increased, the fluorescence intensity of Cu₂S QDs would gradually decreased. The PL spectra in the absence of thiourea showed no fluorescence, indicating that no emissive Cu₂S QDs was obtained without thiourea. The effect of reaction temperatures on the fluorescence spectra of Cu₂S QDs was also investigated (Figure S1c and 1d). The results showed that the maximum PL intensity was obtained at 120 °C. In our synthesis method, S²⁻ produced by the pyrolysis of thiourea was used as the precursor of sulfur (**Equation S1**). When the temperature was lower than decomposition temperature of thiourea, Cu₂S QDs could not be synthesized successfully. However, if the temperature was too high, Cu₂S QDs would precipitated rapidly due to excessive growth and had no fluorescence. The PL spectra and PL intensity of Cu₂S QDs synthesized with different reaction time showed that the PL intensity increased with reaction time extended, reaching the maximum at 30 min, and then decreased with the further extension of reaction time (Figure S1e and 1f). The effect of the reaction pH on the PL intensity were also studied. As shown in Figure S1g and 1h, the PL intensity increased with the increase of pH values and reached the maximum at pH 5, then decreased with further increase of pH. These may be attributed to the different existence forms of GSH as ligand at different pH conditions.



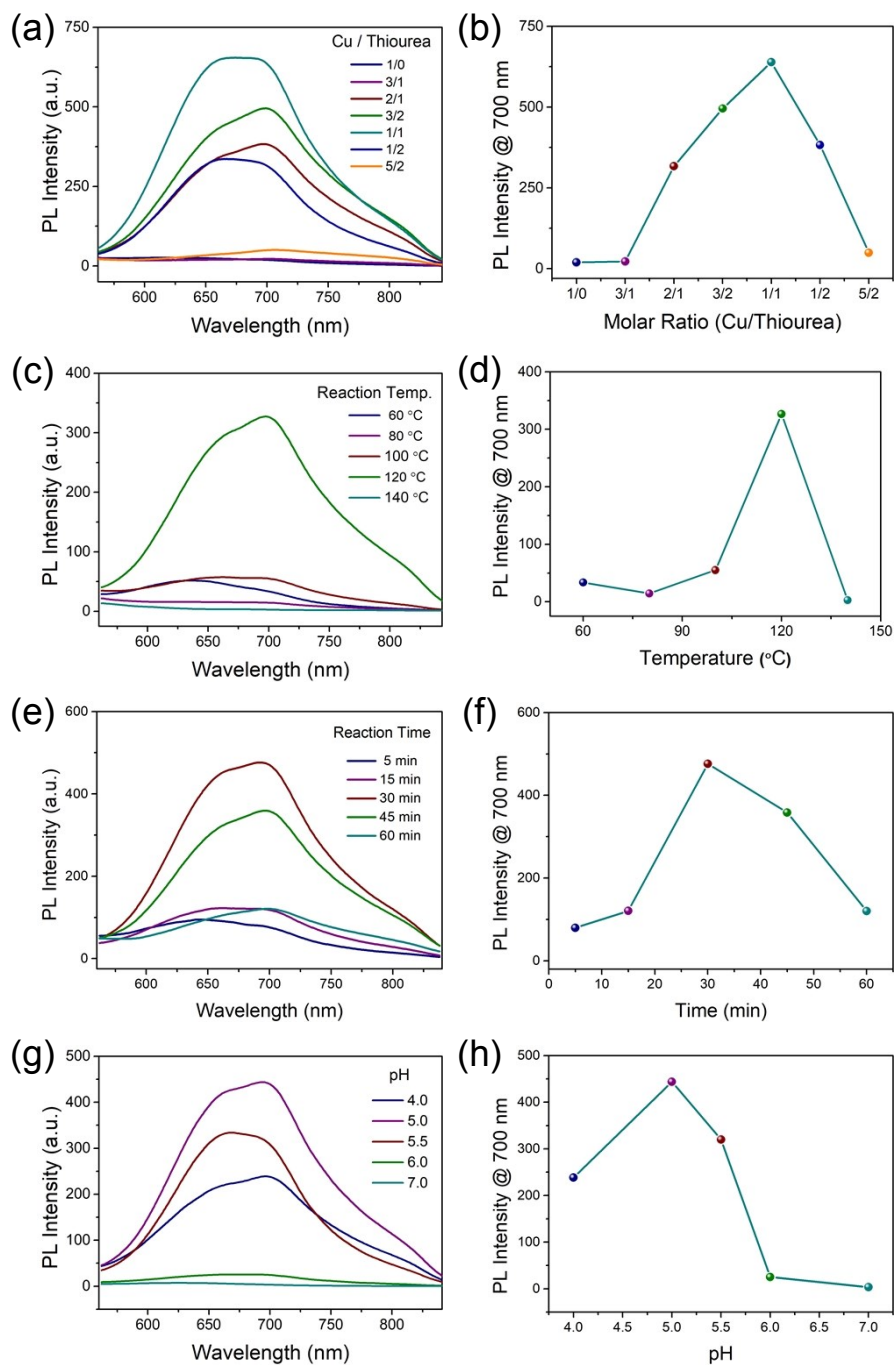


Figure S1. Effects of (a, b) Cu²⁺/thiourea molar ratio, (c, d) reaction temperature, (e, f) time and (g, h) pH on the fluorescence spectra and intensity of Cu₂S QDs.

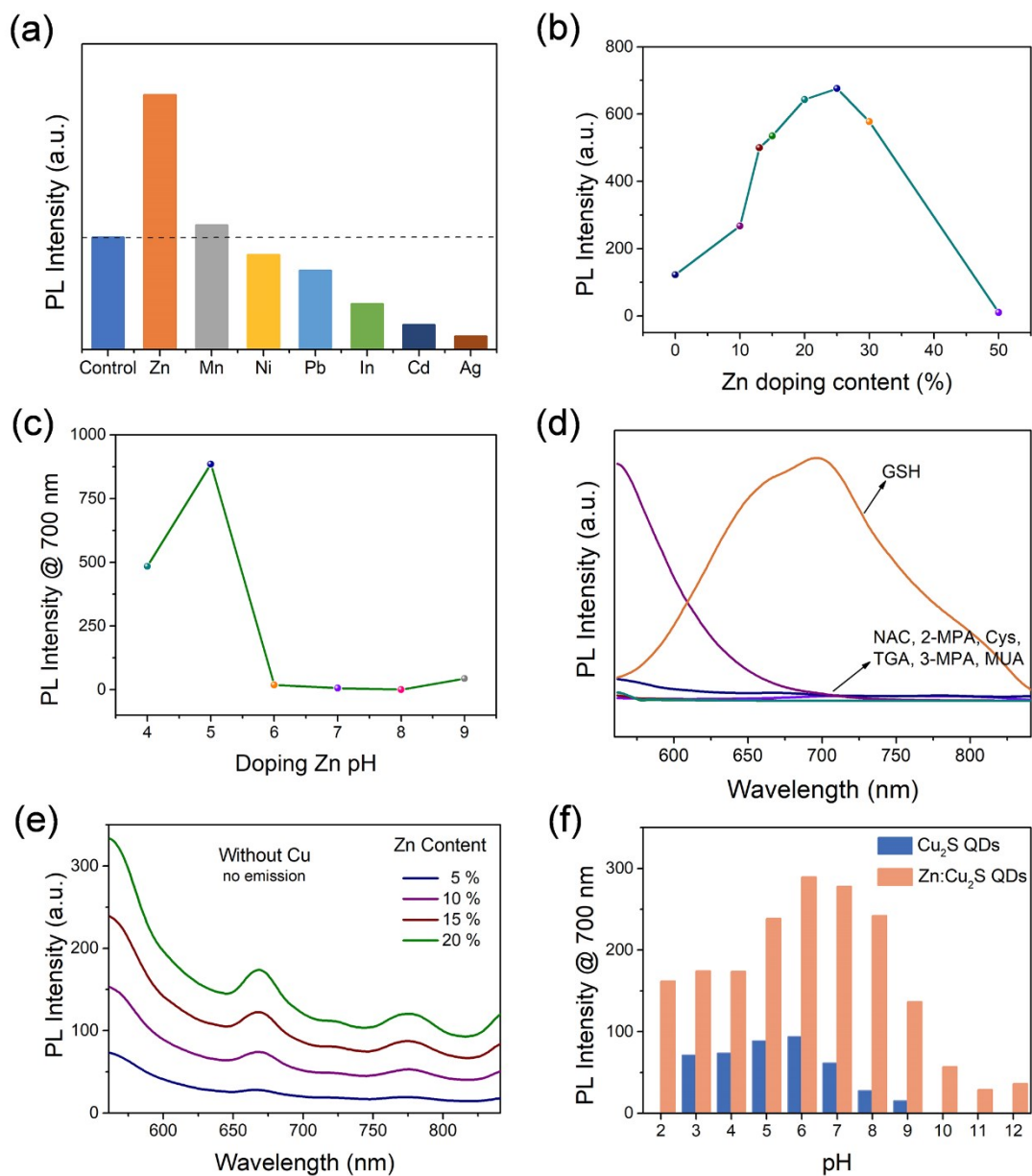


Figure S2. The effect of (a) different doping transition metal ion, (b) Zn content and (c) doping pH on fluorescence intensity of Zn:Cu₂S QDs. (d) The PL spectra of the products synthesized with different surface ligands. (e) The PL spectra of the products synthesized without Cu precursors. (f) The PL intensity of Cu₂S and Zn:Cu₂S QDs at different pH.

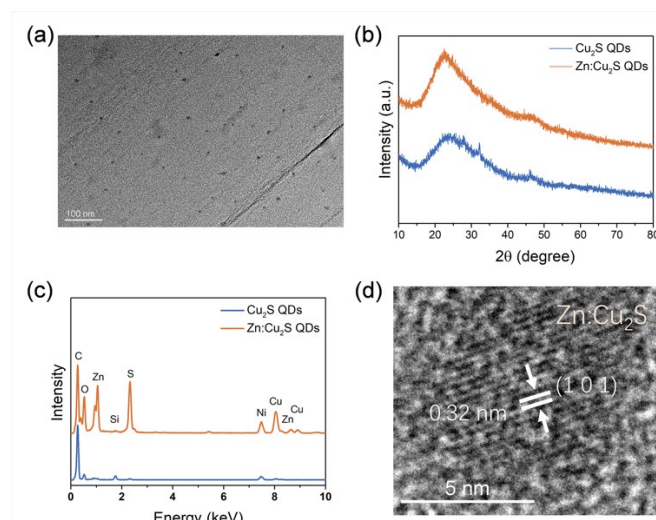


Figure S3. (a) The representative TEM images of Cu_2S QDs and (b) XRD patterns and (c) EDX of the Cu_2S QDs and $\text{Zn}:\text{Cu}_2\text{S}$ QDs. (d) HRTEM image of $\text{Zn}:\text{Cu}_2\text{S}$ QDs.

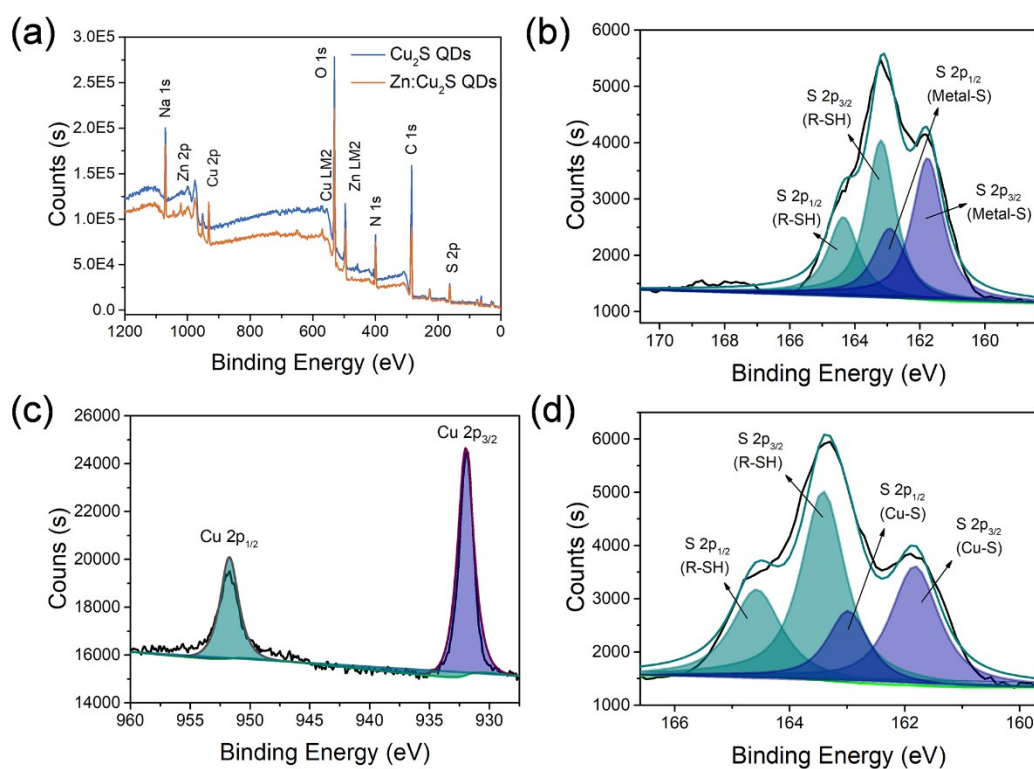


Figure S4. High-resolution XPS spectra of (a) summary, (b) S 2p in $\text{Zn}:\text{Cu}_2\text{S}$ QDs, (c) Cu 2p and (d) S 2p in Cu_2S QDs.

First-order reaction integral rate equation function

$$I_{Z,n} = I_{Z,0} e^{-k_1 n} \quad \text{(Equation S2)}$$

Where $I_{Z,0}$, $I_{Z,n}$ are defined as PL intensity of Zn:Cu₂S QDs before and after n times excitation, and k_1 is photoactivation rate constant.

Lifetime bi-exponential function

$$I(t) = A_1 e^{-t/\tau_1} + A_2 e^{-t/\tau_2} \quad \text{(Equation S3)}$$

$$\tau_{av} = (A_1 \tau_1^2 + A_2 \tau_2^2) / (A_1 \tau_1 + A_2 \tau_2) \quad \text{(Equation S4)}$$

Where τ_1 , τ_2 are defined as lifetimes, A_1 , A_2 are corresponding pre-exponential factors, respectively and τ_{av} calculated by **Equation S4** represents the average lifetime of Cu₂S QDs.

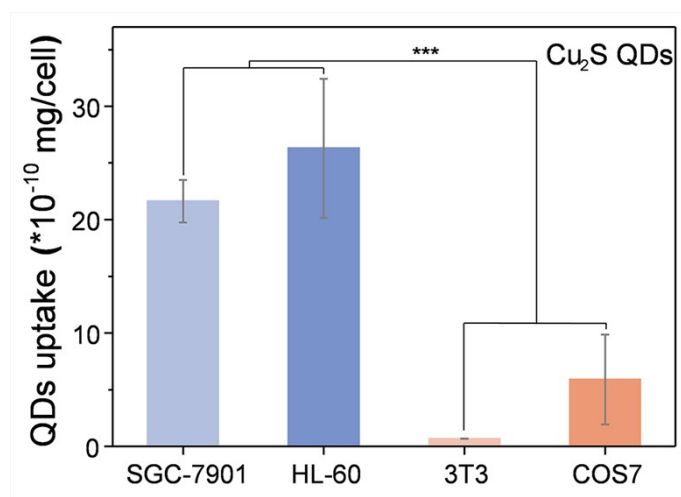


Figure S5. Intracellular Cu contents of SGC-7901, HL-60 and 3T3, COS7 cells treated with Cu₂S QDs for 24 h (n = 3) (Statistical analysis was based on Student's t test: *** $P < 0.001$).

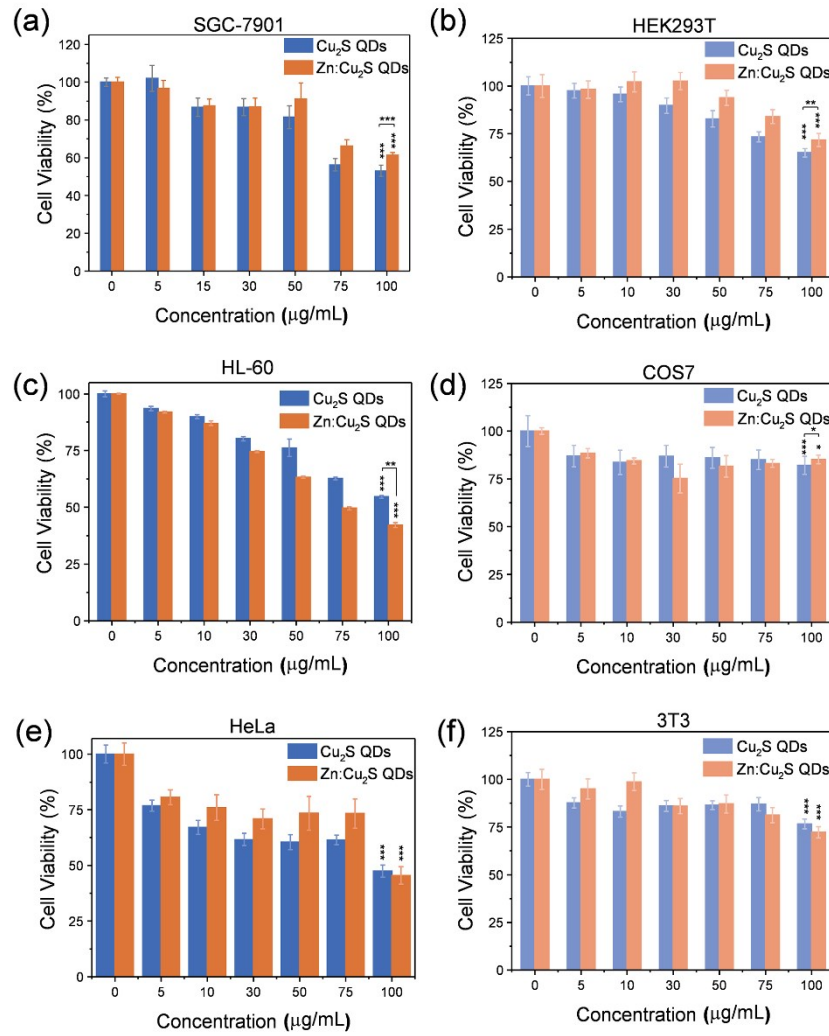


Figure S6. MTT results of normal cells (a, c and e) and tumor cells (b, d and f) incubated with Cu_2S and Zn: Cu_2S QDs for 24 h at different concentrations. (* $P < 0.05$, ** $P < 0.01$, *** $P < 0.001$)

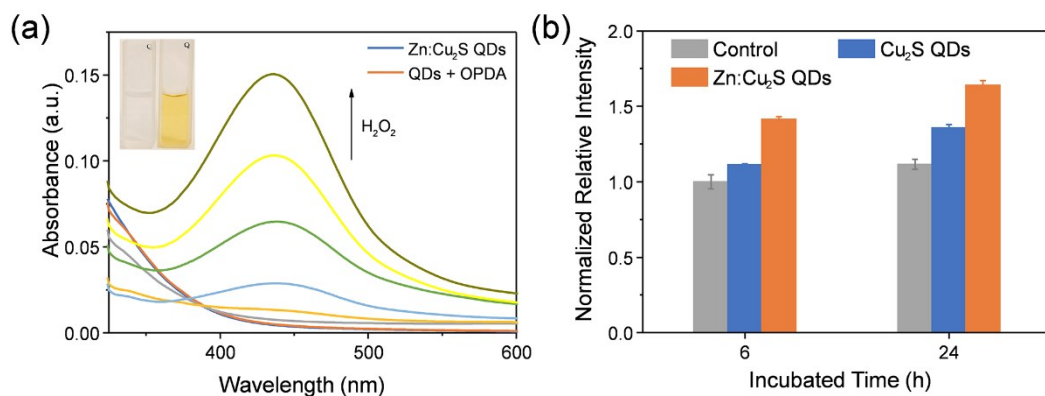


Figure S7. (a) UV-vis spectra and photographs (inset) of Zn:Cu₂S QDs solution treated with OPDA and OPDA plus H₂O₂, (b) The relative ROS intensity of SGC-7901 cells after incubated with Zn:Cu₂S QDs for different time.

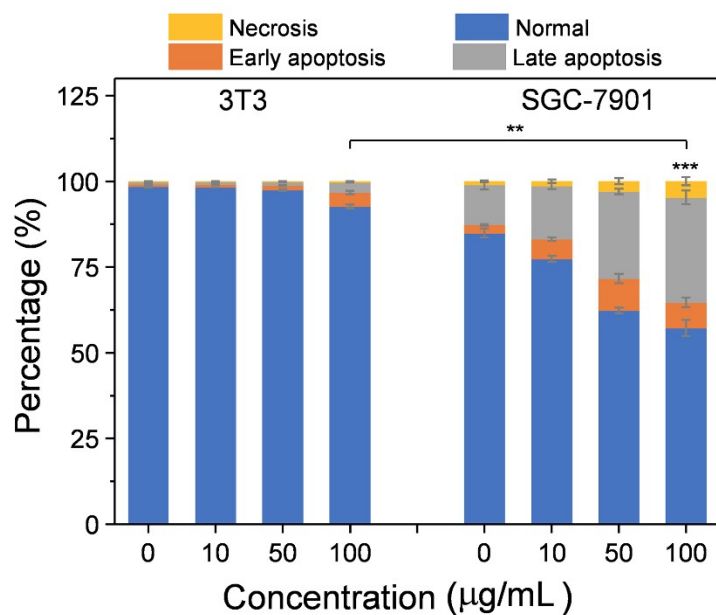


Figure S8. Histogram of apoptosis after incubated with Zn:Cu₂S QDs for 24 h (** $P < 0.01$, *** $P < 0.001$).

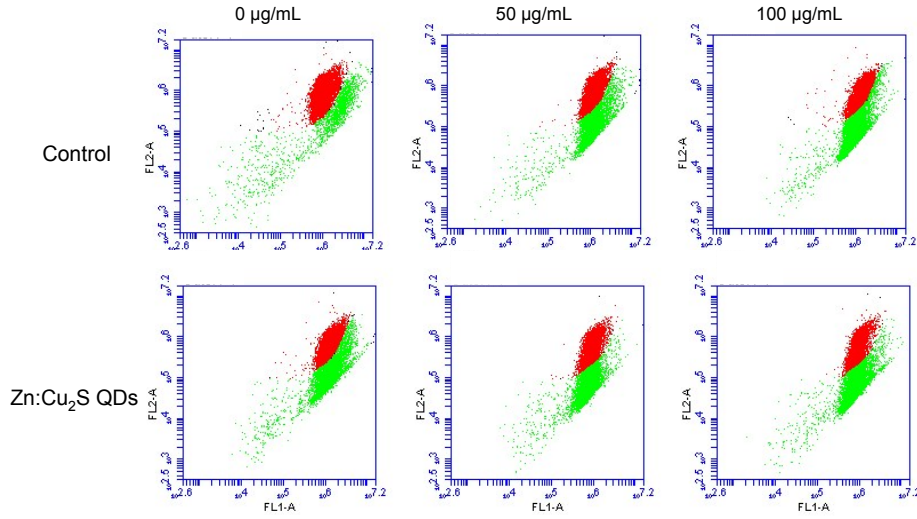


Figure S9. Flow cytometry analysis of mitochondrial membrane potential of SGC-7901 cells after treated with or without Zn:Cu₂S QDs at different concentration for 24 h.

Table S1. Mitochondrial transmembrane potential assay of Cu₂S QDs.

Cells		Control	Cu ₂ S (µg/mL)		
			25	50	100
P _{Red}	SGC-7901	1.00 ± 0.35	0.91 ± 0.06	0.50 ± 0.02	0.39 ± 0.02
P _{Green}	3T3	1.00 ± 0.36	0.84 ± 0.09	0.78 ± 0.10	0.87 ± 0.04

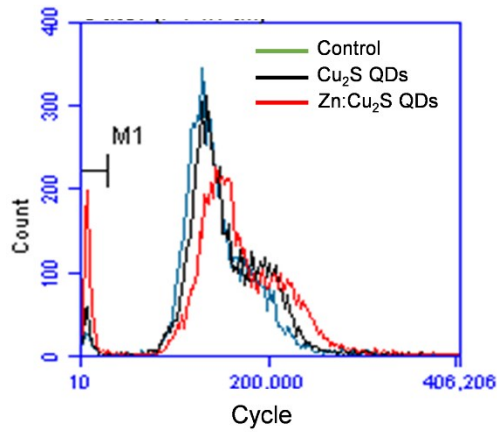


Figure S10. Flow cytometry analysis of cycle of SGC-7901 cells after treated with Cu_2S and $\text{Zn}:\text{Cu}_2\text{S}$ QDs for 24 h.

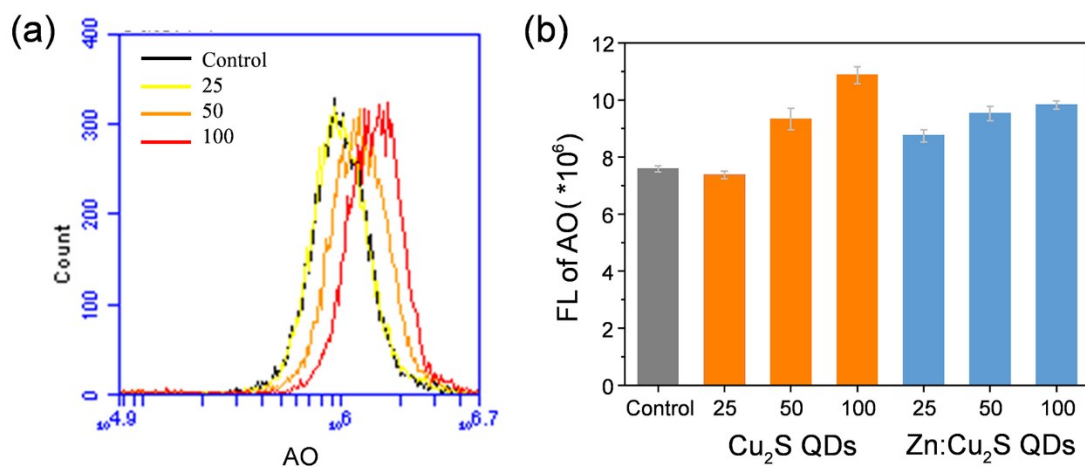


Figure S11. (a) The Cu_2S QDs treated 24 h and (b) summary analyse of AO staining SGC-7901 cells by flow cytometry.

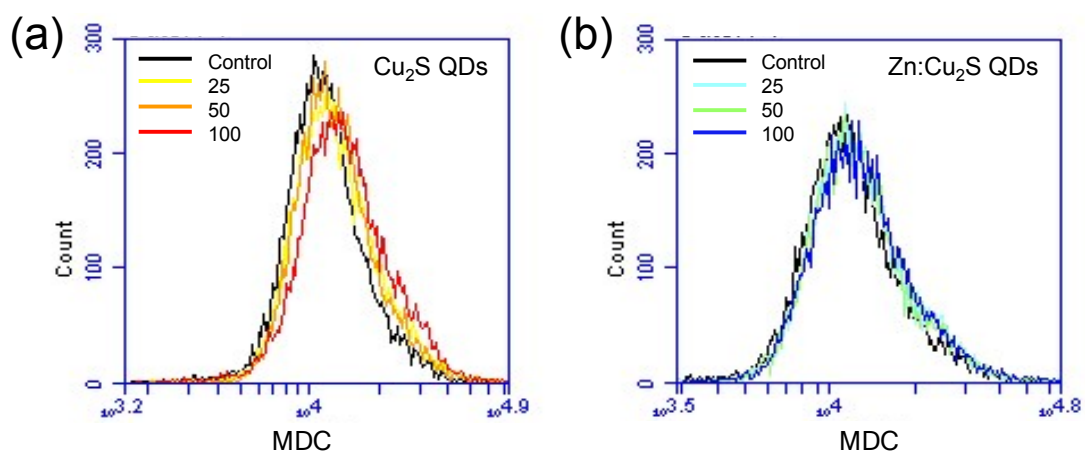


Figure S12. Flow cytometry analysis of MDC staining SGC-7901 cells after treated with (a) Cu₂S and (b) Zn:Cu₂S QDs for 24 h.

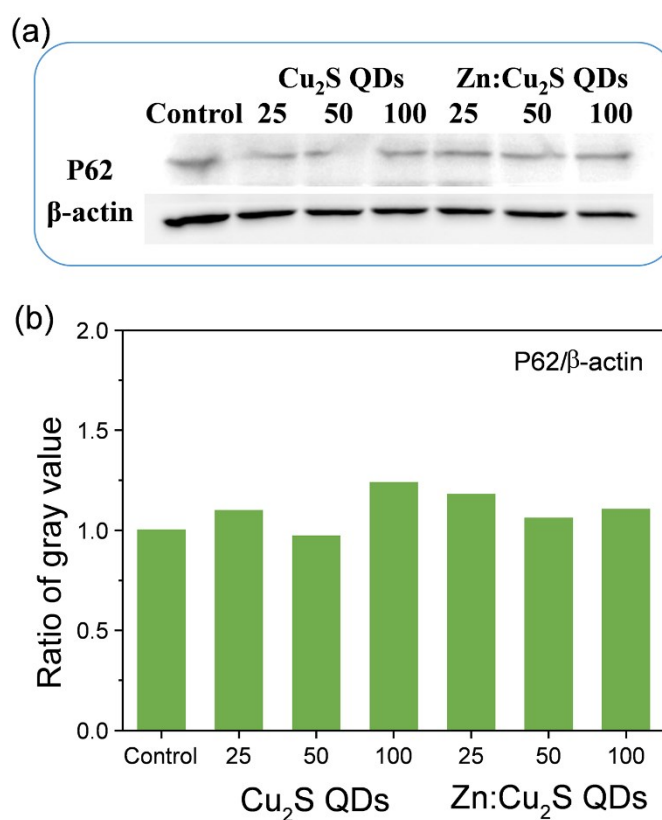


Figure S13. Western blot analysis of P62 protein in SGC-7901 cells after different treatments taking β -actin as a reference.

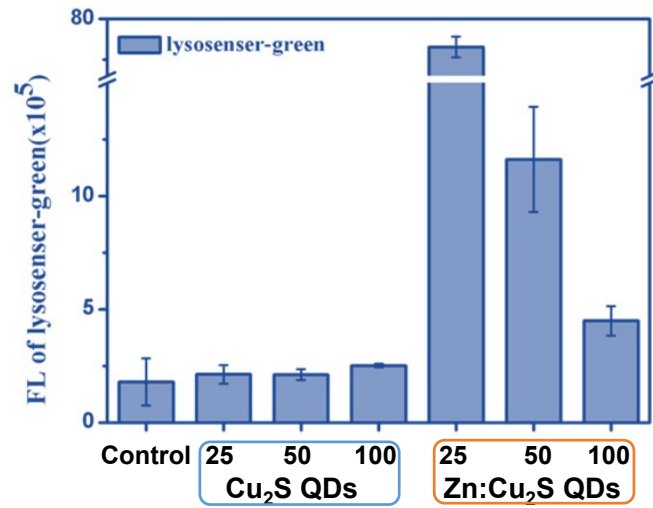


Figure S14. LysoSensor-Green staining of SGC-7901 cells after treatment with Cu₂S and Zn:Cu₂S QDs for 24 h.

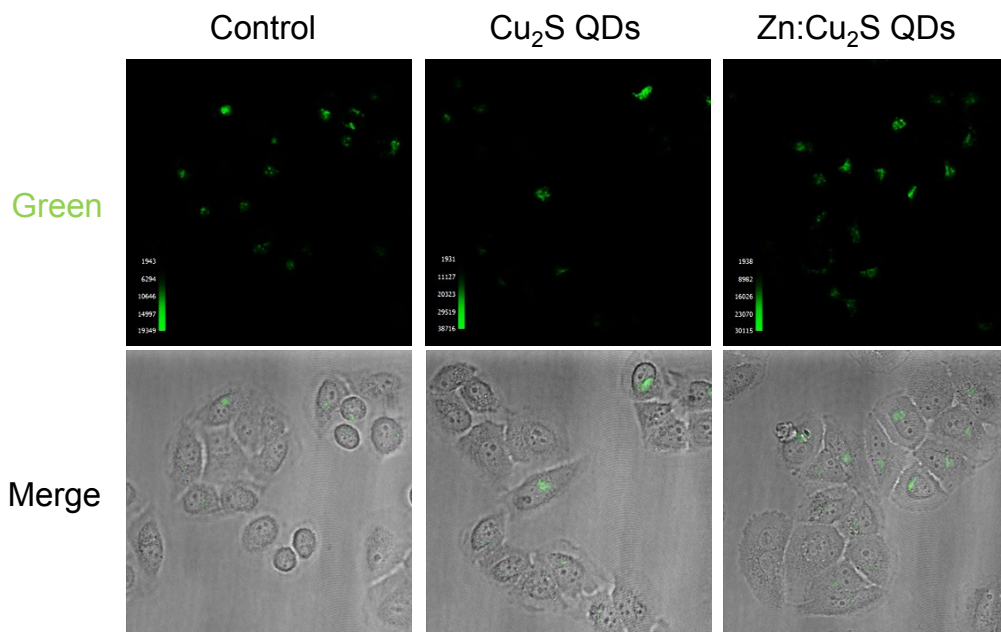


Figure S15. Confocal microscopy analysis of LysoSensor-Green stained SGC-7901 cells after treatment with 100 µg/mL Cu₂S and Zn:Cu₂S QDs for 24 h.

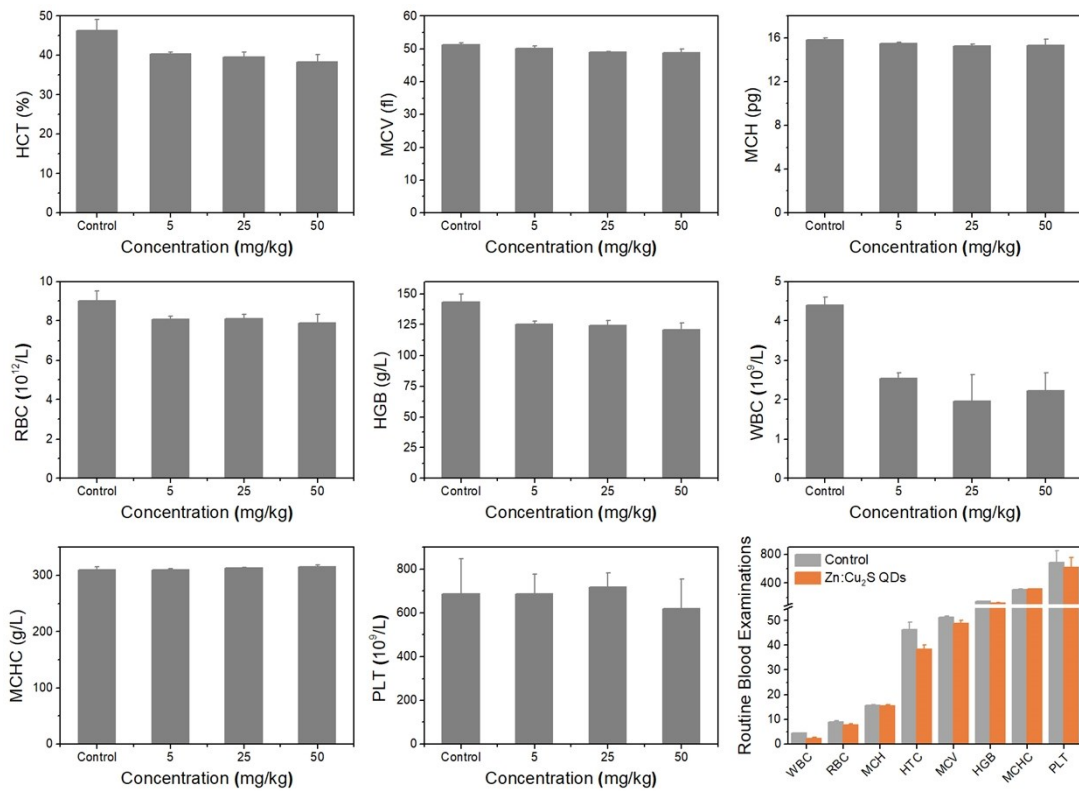


Figure S16. Hematological assay. The related indexes of mice from each group at different Zn:Cu₂S QDs doses of 0 mg kg⁻¹, 5 mg·kg⁻¹, 25 mg·kg⁻¹ and 50 mg·kg⁻¹ after axillary subcutaneous administration and further 15 days feeding.

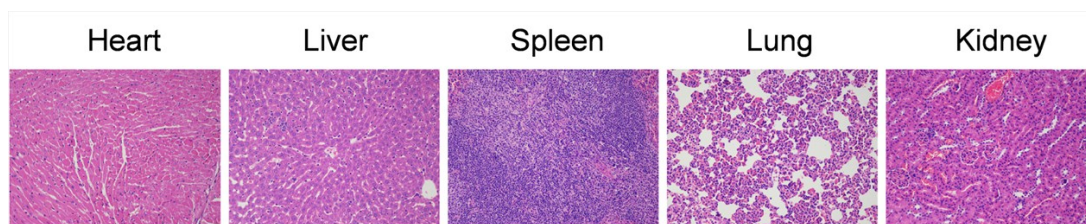


Figure S17. Histological analyses of the major tissues for systemic toxicity analysis at Zn:Cu₂S QDs doses of 50 mg·kg⁻¹.